

# Cyclic Performance of Buckling Restrained Composite Braces Composed of Selected Materials

A.R. Rahai<sup>1,\*</sup>, M. M. Alinia<sup>2</sup>, S. M. F. Salehi<sup>3</sup>

Received: March 2007, revised: July 2008, accepted: November 2008

**Abstract:** Concentric bracing is one of the most common lateral load resistant systems in building frames, and are applied to many structures due to their manufacturing simplicity and economics. An important deficiency in the bracing members is their irregular hysteretic loops under cyclic loading. In order to overcome this problem, it is advised to restrain braces against buckling under compression, since buckling restrained frames dissipate a large amount of energy. One method to restrain braces against buckling is to cover them with concrete. A proper covering can prevent the core from buckling and provide similar capacities whether in tension or compression which would produce regular hysteric curves. In this study, the behavior of buckling restrained braces (BRB) has been investigated by considering different types of surrounding covers. The steel core is encased in concrete with different coverings. The covering types include steel tubes, PVC pipes, and FRP rolled sheets. Experimental and numerical analyses were implemented. According to the results, PVC pipes and FRP sheets are suitable alternatives to steel pipes. Furthermore, the behavior of several types of steel cores was assessed; since, applying steel with high ductility promotes the energy dissipation of the brace. Finally, the effect of the separating layer between the steel core and the concrete on the performance of bracing was evaluated.

**Keywords:** Buckling restrained brace, cyclic behavior, Cumulative ductility, energy dissipation, PVC pipe, and FRP sheets.

## 1. Introduction

Buckling restrained braced framing system (BRB) is recognized as an effective system against sever seismic loads. The common buckling restrained braces (BRBs) and Unbounded Braces (UBs) are formed by encasing a steel cross-shape or a flat bar member core with a steel tube confined with infill concrete (see Fig. 1). The steel core can elongate independent of the encasing. In such bracing system, the core is designed to yield in both tension and compression cases. Encasing the core avoids compression buckling. Unbonding material such as silicone sheet, asphalt paint, vinyl sheet and butyl rubber should be placed around the steel core before placing the mortar [1]. The isolator layer causes the core to act independent of the concrete and consequently, regular hysteric curve

is obtained. In addition, cores normally reach higher modes and absorb more energy. Figure 2 depicts a comparison between the hysteric

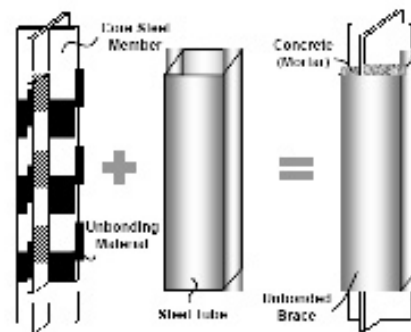


Fig. 1 Schematic of buckling restrained brace [5]

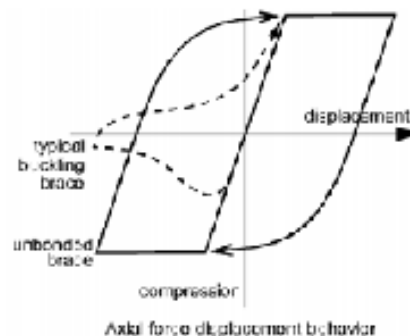


Fig. 2 Behavior of conventional versus buckling-restrained brace [4]

\* Corresponding author: fax: 021-6647921, Email: rahai@aut.ac.ir

<sup>1</sup> Professor, Department of Civil Engineering, Amirkabir University of Technology, Phone: 021 – 64542030.

<sup>2</sup> Professor, Department of Civil Engineering, Amirkabir University of Technology, Phone: 021 – 64543232, E-mail: m.alinia@aut.ac.ir

<sup>3</sup> M.Sc., Department of Civil Engineering, Amirkabir University of Technology, Phone: 021 – 88663405, E-mail: sanam\_salehi\_m@yahoo.com

behaviors of BRB and ordinary braces. If the buckling resistant mechanism is designed appropriately, the core would yield in compression and exhibit similar tension and compression strengths. It would also perform a regular hysteric behavior up to 2% strain [2].

Early research on BRBs was carried out by Yoshino et al. [3]. They did some cyclic tests on two specimens called "Shear wall with braces", consisting of a flat steel plate encased by reinforced concrete panels with some nonbonding materials between them. One specimen had a clearance of 15mm between the lateral sides and the surrounding panel while the other did not have any spacing. The former exhibited higher deformation and energy dissipation capacity than the latter.

Wakabayashi et al. [1] developed a system in which braces made of steel flat plates were encased by reinforced concrete panels with an unbonding layer between them. They found that the process of achieving nonbonding was very important to make the brace-panel system satisfy the condition in which only the brace would resist horizontal loading, while the concrete panel served only to prevent the brace from buckling.

Siridhara introduced sleeved column as a BRB [4]. The idea was to decouple the compression load resistant of the core from the flexural buckling resistance of sleeve. In a sleeve column, the core is loosely placed inside a sleeve and the load is applied directly to the core.

The first test on steel braces encased in mortar-infilled steel tubes was conducted by Kimura et al. [5]. Although there was no nonbonding material or gap between the mortar and braces, the mortar-infilled tube showed some effects on restraining the cores against buckling. In a subsequent research [6], four full-scale specimens were tested under cyclic loading. They concluded that if the ratio between the Euler's limit of outer tube and yielding strength of brace were larger than 1.9, no buckling would have occurred in the core braces and that specimens showed good hysteretic behavior.

Iwata et al. [4] reviewed the cyclic performance of some commercially available BRBs in Japan. Three large-scale unbounded braces were tested at the Berkeley University to

help the design and construction of buildings with BRBs. Black et al [7] carried out various analyses to investigate the stability of the interior core in the higher vibrational modes and the elastic torsional buckling of the core. Higgins and Newell [4] studied a type of BRB that used a steel pipe filled with noncohesive media as the buckling-restrained mechanism; graded aggregates were used as the noncohesive media. Chen (2001) found out that applying low strength steel will make the brace yield with less deflection and reach more ductility [4].

Tsai and Lai (2003) studied the effect of isolators on the cyclic response of braces. The tests results illustrated that the silicone rubber sheet of 2 mm thickness caused a minimum difference between the tension and compression strength and was the optimum condition [8]. Sabelli (2003) evaluated the seismic demand of frames with covered bracing systems [9]. According to the research performed by Mayes and Goings, this type of brace improved the performance level of structures [10]. In the study carried out by Uang (2003), the advantages of applying BRBs in dual systems for reducing permanent deflections were inspected [11]. Kim et al [12- 14], introduced a seismic design procedure for BRBF based on energy dissipation and direct displacement design procedure.

## 2. Specimens' properties

In this research, the behavior of BRBs is studied with regards to employ different surrounding cover materials. The work is carried out by both numerical Finite Element and experimental methods. Due to the laboratory instrumental limitations, the specimens were scaled down about 7 times.

Furthermore, the effect of the material characteristic of the core on the behavior of braces has been investigated. For this purpose, the Finite Element method was utilized on a real size model.

### 2.1 Geometrical properties of the specimens

Cores with different sizes were considered to investigate the behavior of the bracings having



Fig. 3 Dimensions of model

Table 1 Cover dimensions

Model	Diameter of Concrete(mm)	Tube Material	Tube Thickness
Model 1	90	-	-
Model 2	90	Steel	3
Model 3	90	PVC	4.3
Model 4	90	G-FRP	1 layer

various covers as shown in figure 3. In order to scrutinize the effect of different coverings on the behavior of BRBs, four specimens, the characteristics of which are given in table 1, were considered. The surrounding cover was assumed to be 600 mm away from two ends.

To inspect the effect of core material characteristic on the behavior of braces, the dimensions of the core were enlarged 7 times than those given in figure 3 and its thickness was assumed to be 19 mm. The cover was made of steel having 250 by 250 by 6 mm dimensions.

## 2.2 Mechanical properties of specimens

The fabricated specimens consisted of interior cores, isolator layers, surrounding covers, and in-filled concrete. The cores were made of normal mild steel material. Based on the direct tension test of the standard steel specimen, the yield and rupture stress were 258 MPa and 439.9 MPa respectively.

Table 2 gives the characteristics of the models tested for the inspection of the effect of core material on the brace behavior. Since there was no available test for evaluating hardening effects,

Table 2 Properties of steel

Steel	E (GPa)	F <sub>y</sub> (MPa)	F <sub>u</sub> (MPa)	Ultimate strain%
Carbon steel	200	240	375	20
High-Strength, Low-Alloy Carbon	200	346	470	17
Heated-Treated Structural Alloy Steel	200	692	762	7

it was assumed that 1% of the primary elastic modulus, to FEMA [15], should be accounted for.

The fabricated concrete had a density of  $23.6 \text{ kN/m}^3$ , a 100 mm slump, and a compressive strength of 24 MPa. The same quantities were assumed in the Finite Element method of analysis. According to ACI, elastic modulus and rupture strength of concrete is presumed as follows [16]:

$$f_r = 0.7\sqrt{f'_c} = 3.4 \text{ MPa} \quad (1)$$

$$E = 4700\sqrt{f'_c} = 23 \text{ GPa} \quad (2)$$

The layer acting as the isolator between the concrete and steel was a polymeric substance named Butel Rubber which had low frictional resistance and a high plastic attribute. The frictional coefficient was assumed to be 0.1 for the foregoing material in the models.

Since the main objective of this study was to investigate the effect of different cover materials, three types of covers, normally mild steel, FRP sheets, and PVC pipes were prepared for tests. The FRP was made of E-Glass mat fibers with the density of  $200 \text{ gr/m}^2$ . The PVC pipe employed in the experiment was of a high pressure type of 4.3 mm thickness and the Young's modulus of 3 GPa. The tensile and compressive strength and rupture strains were 55 MPa, 88 MPa, and 30%, respectively.

## 3. Specimen fabrication and test setup

At first, the steel core was cut as illustrated in figure 3, and the core was covered by the isolator layer. Special steel-rubber glue was used to bond the butyl rubber to the steel. For this purpose, the bonding surfaces had to be cleaned from dirt. Then, the framework and concrete casting were put on. While casting the concrete, sufficient attention was given to the core position which had to be settled in the center of the core framework. The specimens were kept in water and slaked lime for 28 days. In order to prevent the steel from rusting in the specimen, its surface was coated with a single layer of paint. Then the specimens were brought out of the moisture, one of the specimens was wrapped with FRP

composite. The FRP sheets were manufactured manually by putting the hand-made layers together. The resin used for bonding the FRP to the concrete was made of epoxy and hardener with a relative ratio of 100 to 15. After finishing the bonding process, the specimens were kept in a dry place until the resin was properly dried and the fibers were bonded to the concrete surface. Finally, the specimens were ready to be loaded.

The loading instrument was an “Instron 8502” which can be categorized in the group of head and hydraulic devices. The load could be applied by exerting forces or imposing displacements. The available load and displacement steps were

250kN and 100mm, respectively. The overall view of the device is depicted in figure 4 and 5.

#### 4. Numerical modeling

The modeling was performed using the Finite Element software “ANSYS” [17]. The element “shell 143” was used for the steel core. The stress-strain curve of the steel was assumed to be a bilinear curve. Therefore, the preliminary and secondary elastic modulus and yield stress were used in the analysis. In the models, steel was presumed to have kinematic hardening and concrete was meshed with the element “Solid 65”. The contact element between concrete and steel was used for modeling the unbonding material. This was done in a way that there was a 2.5mm gap between the concrete cover and steel core on each side, so that the core was subjected to the load and could thus reach higher modes, consequently the brace exhibited a better behavior under cyclic loading. The mentioned gap was in fact acting as the thickness of the isolator layer. This unbonding material had to have insignificant frictional coefficient so that the steel could act independently of concrete and exhibited similar tensile and compressive behaviors. Afterward, the surrounding tube was modeled with the element “shell 143” of the ANSYS software.

In order to appropriately model the contact between the concrete and the tube, contact

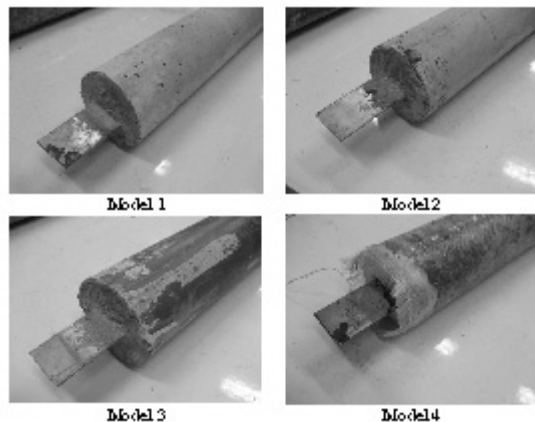


Fig. 4 Test specimen



Fig. 5 Experimental setup for BRB tests

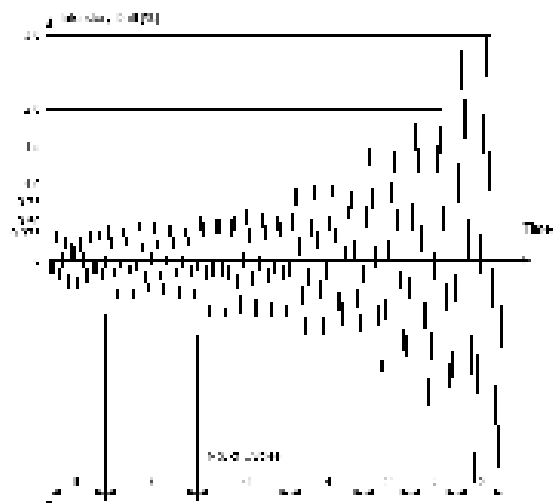
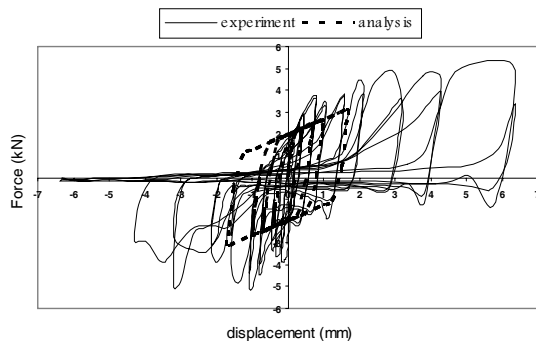


Fig. 6 SAC basic loading history

elements were used in a similar manner. The only difference here was that the contact was assumed to be completely bonded. This meant that all degrees of freedom in steel and concrete were connected together and that no frictional coefficient was needed.

An initial out of plane deformation (warping deformation) was required for analysis. This small initial deformation was in accordance with the buckling mode shape obtained from nonlinear



**Fig. 7** Experimental and analytical cyclic responses of specimen 1

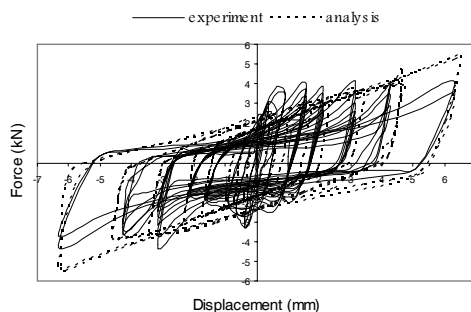


**Fig. 8** Experimental and analytical cyclic responses of specimen 2

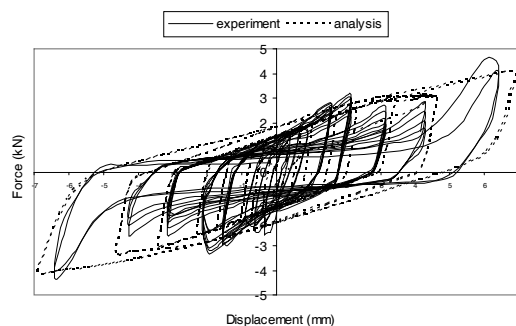


**Fig. 9** Experimental and analytical cyclic responses of specimen 3

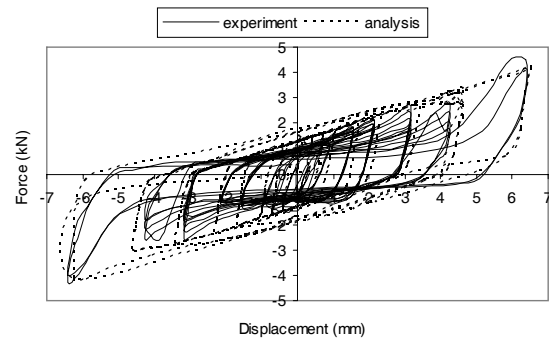


**Fig. 10** Experimental and analytical cyclic responses of specimen 4

buckling analysis [17]. For this purpose, first an Eigen value analysis was carried out. Then the model was subjected to the first mode shape and after the initial deformation, the desired load was applied on the model. Figure 6 shows a typical loading pattern applied to the model.

## 5. Numerical and Experimental results

The results of the carried out tests and finite element analysis are divided into two following sections.

### 5.1. The influence of different surrounding coverings on the behavior of BRB

Figures 7 to 10 depict the hysteretic loops of the specimens. It is illustrated that the hysteretic curve of the specimen whose core was only covered with concrete (no covering), was irregular after a few cycles and its tensile and compressive behaviors were different. The reason is, of course, the low tensile strength of the concrete. The concrete cracked after a few steps and was completely detached from the steel core. In this situation, the core buckled under compressive load and became unstable.

The other three specimens had fairly identical behaviors in tension and compression; and their ultimate bearable deformations were similar. In brief, all three coverings, i.e. steel, FRP and PVC pipe, promoted the cyclic behavior of bracing, prevented the bracing from buckling, and enhanced the energy dissipation during cyclic loading.

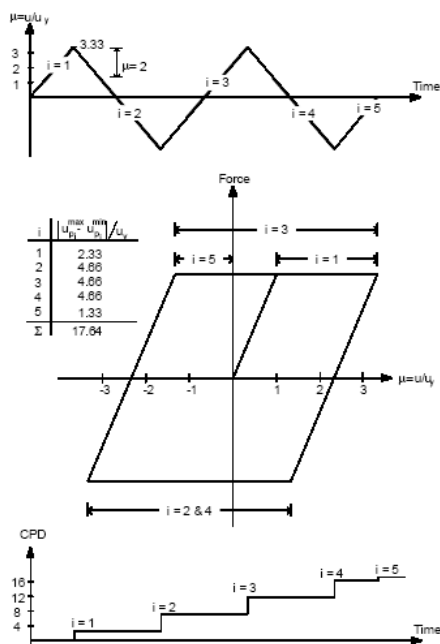


**Fig. 11** The procedure for evaluation of CPD [5]The procedure for evaluation of CPD [5]

Table3 contains the number of bearable cycles and ductility of the each step for all specimens.

Cumulative plastic strain or in other words, cumulative plastic ductility (CPD) is one of the parameters used to express the plastic demand of a covered brace. CPD is the so-called normalized cumulative plastic demand, as given in Eqn. 3:

$$CPD = \sum_i \frac{|u_{pi}^{max} - u_{pi}^{min}|}{u_y} \quad (3)$$

$u_{pi}^{max}$  and  $u_{pi}^{min}$  are the minimum and maximum plastic displacements in each cycle and  $u_y$  is the yield displacement of the brace. Figure11 depicts the calculation of CPD. The first diagram in the figure shows the load history for a specimen. The darker lines represent the part of the load history in which the specimen has undergone the inelastic state. The middle one illustrates the load-displacement loop for the same specimen.

**Table. 4** Dissipated energy

Specimen	Dissipated Energy (J)	$P_{spc} / P_{spc 1}$
1	124.1	1
2	324	2.61
3	260.8	2.1
4	279.5	2.25

Lastly, the lower diagram expresses the CPD versus time, the calculation of which is brought in the table of the figure 11. For the tested specimen, the CPD was calculated through the foregoing method.

In order to calculate the absorbed energy of each specimen, the area under the load-displacement curve was determined and given in Table 4. The surrounding concrete cover adjacent to steel tube, PVC pipe, and FRP sheet respectively caused 160%, 110 % and 125% increase in the dissipated energy of the covered brace in comparison with the uncovered brace. It can be observed that the most dissipation was in the specimen number 2 covered with concrete and steel tube. The PVC pipe and FRP sheet, also, had enhanced significant energy dissipations.

The experimental results somehow differ from the FE analysis. A 10 mm gap between the clamps and covers were inevitable due to test instrument limitations. Therefore after a small

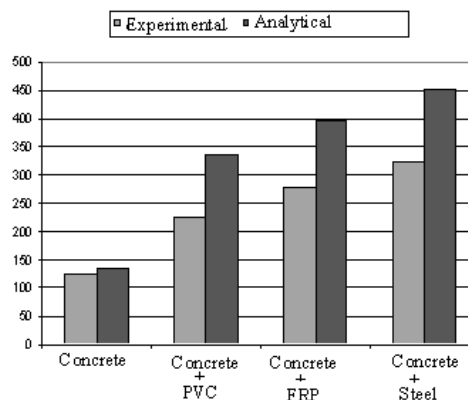


**Fig. 12** The dissipation of energy in experimental and analytical specimen

displacement, the cover reached the test instrument and resumed a false axial strength. As a result, local buckling occurred in those regions. By taking these regions into consideration of the finite element model, however, the analysis did not complete and convergence problems comes up. Therefore, the exposed part of the core was overlooked in the model. In Figure 12, a comparison between the absorbed energy by different specimens for experimental and numerical analysis is presented. The absorbed energy dissimilarity for specimens numbers 2, 3 and 4 is in the order of 30%; whereas, for the

specimen number 1, with concrete cover only, is a little. The reason is that the local buckling that occurred in the exposed region, was not comparable with the overall buckling caused by concrete cracking; as a result, the experimental test specimen suffered by the overall buckling before local buckling occurred and that the behavior was the same as the numerical model.

To add up, the polymeric materials such as PVC pipes and FRP sheets can be appropriate substitutions for the steel tube in brace covering and can be utilized in situations.

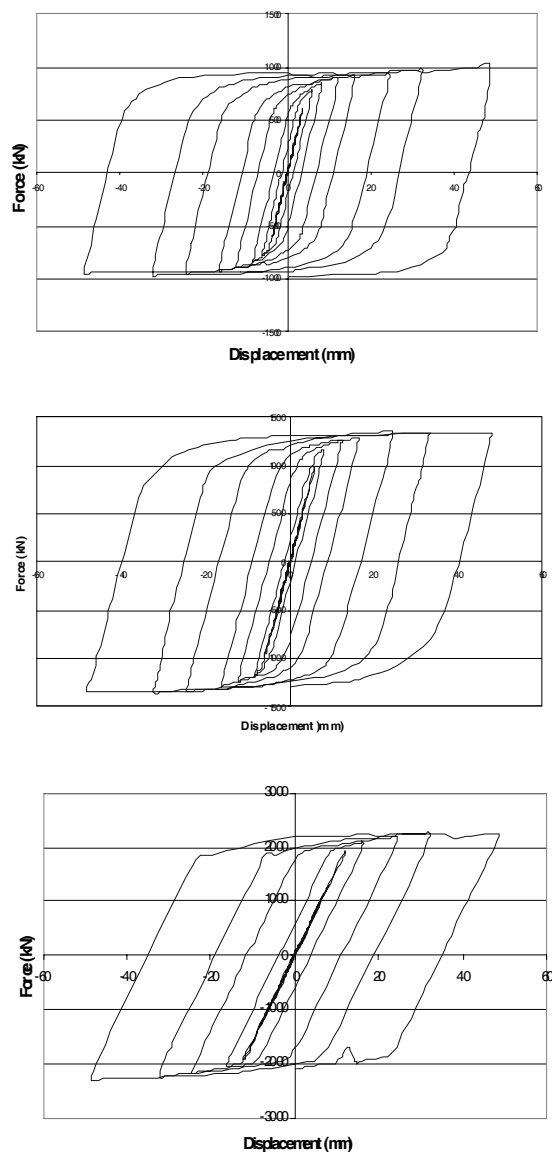


Fig. 13 Hysteretic loops; (From Top): Carbon steel, high strength, heat treated

## 5.2 The effect of core steel characterization on the BRB behavior

In steel structure constructions, depending on the desired structure performances regarding strength and ductility, different types of steel are used. In this study, three common types of steel commonly, normal mild steel, high strength low alloy carbon steel, and heat-treated structural

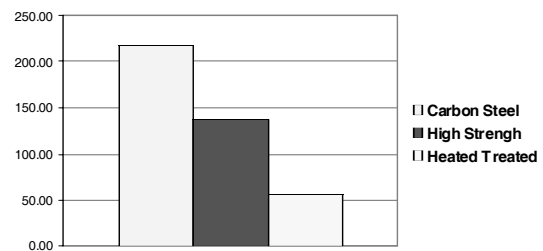


Fig. 14 The values of CPD

alloy steel, were used for inspecting the effect of steel core material on the behavior of the BRB and the corresponding hysteric curves, have been drawn in Figure13. In order to accurately examine the behavior of bracing core under repeated loading without the influences of other factors, the unbonding layer was presumed to be ideal with inconsiderable friction between the core and the concrete. Figure 13 contain the hysteric curves of BRB, with three different steels. Comparison between the three specimen show that all three curves were regular curves and that all specimens were capable to bear the applied cyclic load. Their difference is the generated force in the brace due to the applied deformation and accordingly their inelastic deformation and CPD. The trends of CPD variations for different specimens are brought in Figure14.

According to the result, normal mild steel has the most CPD; hence, it is a high energy dissipater and has appropriate seismic behavior. Despite the fact that the total applied cyclic load was bearable by the other two specimens, the brace was mostly in elastic state, given low energy dissipation.

It is understood from the preceding diagram that the mild steel core has the most CPD and

high energy dissipation whereas its absorbed energy is less than the other two specimens. Hence, depending on the expected behavior of the brace, different types of steel can be considered for the core.

## 6. Conclusions

Specimens with concrete, steel, and FRP covers have similar cumulative plastic ductility (CPD) and bearable load cycles, while the specimen with only concrete cover buckles under compression after only a few cycles and exhibits no plastic ductility in compressive region. All three covers, i.e. Steel tube, FRP sheet and PVC tube, have high energy dissipation and enhance the performance of the brace. Therefore, it can be concluded that the polymeric materials such as PVC pipes and FRP sheets are possible substitutes for steel tubes, depending on the circumstances. Another influencing factor in energy dissipation of braces is the characterization of the steel core. According to the results, applying mild steel produces high CPD in the structure, while the area under load-displacement for high strength steels is more and consequently they absorb more energy.

## References

- [1] Xie, Q., "State of the buckling-restrained braces in Asia", *Jurnal of Constructional Steel Research*, 61, 2005, 727-748.
- [2] Atsushi, W., Yasuyoshi, H., Eiichiro, S., Akira, W., Morhisa, F. "Properties of Brace Encased in Buckling-Restraining Concrete and Steel Tube", *Proceedings of 9th World Conference on Earthquake Engineering*, Tokyo-Kyoto, Japan, vol.4, 1988, pp. 719-24.
- [3] Yashino T, Karino Y., *Experimental study on shear wall with braces: Part 2. Summaries of technical papers of annuals meeting*, vol. 11. Architectural Institute of Japan Engineering Section; 1971. p. 403-4 [in Japanese].
- [4] Uang, C. M. and Nakashima, M., *Buckling-Restrained Braced Frames*, CRC, 2004.
- [5] Kimura K., "Tests on braces encased by mortar-infilled steel tubes", *summaries of technical papers of annual meeting*. Architectural Institute of Japan; 1967. p. 1041-2.
- [6] Mochizuki, *Experimental study on precast concrete shear walls- Part6. Summaries of technical papers of annual meeting*. Architectural Institute of Japan; 1979. p 1677-8.
- [7] Black, C., Makris N, Aiken I. "Component Testing, Stability Analysis and Characterization of Buckling-Restrained Unbounded Braces", *Pacific Earthquake Engineering Research Center College of Engineering, University of California, Berkeley*, 2002.
- [8] Lai, J.W., Tsai, K.C., "Research and Application of Buckling Restrained Braces in Taiwan", [www.Google.com](http://www.Google.com).
- [9] Sabelli R., "Seismic demand on steel braces frames building with buckling-restrained braces", *Engineering Structure*, 25, 2003, 655-666.
- [10] Min, L.L., Tsai K., Hsiao.P., "Compressive Behavior of Buckling-Restrained Brace Gusset Connections", *First International Conferences on Advances in Experimental Structure Engineering*, AESE 2005, Japan, 2005.
- [11] Uang, C.M., Kiggins, Sh., "Reducing Residual Drift of Buckling-Restrained Braced Frames as a Dual System", 2004, [www.elsevier.com](http://www.elsevier.com).
- [12] Kim, J., Seo, Y., "Seismic design of low-rise frames with buckling-restrained braces", *Engineering Structure*, 26, 2004, 543-551.
- [13] Kim, J., Choi, H., "Behavior and design of structures with buckling-restrained braces", *Engineering Structure*, 26, 2004, 693-706.
- [14] Choi, H., Kim, J., "Energy-based seismic design of buckling-restrained braces frames using hysteretic energy spectrum", *Engineering Structures*, 28, 2006, 304-311.
- [15] FEMA, "NEHRP guidelines for seismic rehabilitation of buildings (FEMA273)", Washington, D.C., 1997.
- [16] ACI318, *Building Code Requirement for Structural Concrete (ACI 318-02)*, American Concrete Institute, International Committee 318, 2002.
- [17] ANSYS 6.1, "Reference Manual", Published by Ansys Inc.